





A chromosome scale tomato genome built from complementary PacBio and Nanopore sequences alone reveals extensive linkage drag during breeding

Willem M. J. van Rengs^{1,†}, Maximilian H.-W. Schmidt^{2,†}, Sieglinde Effgen¹, Duyen Bao Le³, Yazhong Wang¹, Mohd Waznul Adly Mohd Zaidan¹, Bruno Huettel⁴ , Henk J. Schouten⁵ , Björn Usadel^{2,3,*}  and Charles J. Underwood^{1,*} 

¹Department of Chromosome Biology, Max Planck Institute for Plant Breeding Research, Carl-von-Linné-Weg 10, 50829, Cologne, Germany,

²IBG-4 Bioinformatics, Forschungszentrum Jülich, 52428, Jülich, Germany,

³Heinrich Heine University Düsseldorf, Institute of Biological Data Science, Düsseldorf, Germany,

⁴Max Planck-Genome-center Cologne, Carl-von-Linné-Weg 10, 50829, Cologne, Germany, and

⁵Department of Plant Breeding, Wageningen University and Research, P.O. Box 386, 6700, AJ, Wageningen, The Netherlands

Received 18 November 2021; revised 19 January 2022; accepted 24 January 2022

*For Correspondence (e-mail b.usadel@fz-juelich.de; cunderwood@mpipz.mpg.de.)

[†]These authors contributed equally to this work.

SUMMARY

The assembly and scaffolding of plant crop genomes facilitate the characterization of genetically diverse cultivated and wild germplasm. The cultivated tomato (*Solanum lycopersicum*) has been improved through the introgression of genetic material from related wild species, including resistance to pandemic strains of tobacco mosaic virus (TMV) from *Solanum peruvianum*. Here we applied PacBio HiFi and ONT Nanopore sequencing to develop independent, highly contiguous and complementary assemblies of an inbred TMV-resistant tomato variety. We show specific examples of how HiFi and ONT datasets can complement one another to improve assembly contiguity. We merged the HiFi and ONT assemblies to generate a long-read-only assembly where all 12 chromosomes were represented as 12 contiguous sequences (N50 = 68.5 Mbp). This chromosome scale assembly did not require scaffolding using an orthogonal data type. The merged assembly was validated by chromosome conformation capture data and is highly consistent with previous tomato genome assemblies that made use of genetic maps and Hi-C for scaffolding. Our long-read-only assembly reveals that a complex series of structural variants linked to the TMV resistance gene likely contributed to linkage drag of a 64.1-Mbp region of the *S. peruvianum* genome during tomato breeding. Through marker studies and ONT-based comprehensive haplotyping we show that this minimal introgression region is present in six cultivated tomato hybrid varieties developed in three commercial breeding programs. Our results suggest that complementary long read technologies can facilitate the rapid generation of near-complete genome sequences.

Keywords: *Solanum lycopersicum*, *Solanum peruvianum*, PacBio, SMRT sequencing, Oxford Nanopore Technologies, Nanopore sequencing, genome assembly, linkage drag, plant breeding, tobacco mosaic virus.

INTRODUCTION

DNA sequencing technology has evolved rapidly in the last two decades, and long read DNA sequencing has fundamentally altered approaches in genome assembly. Long DNA sequence reads that can span repeated sequences, including the full length of transposable elements, can simplify the assembly process (Dumschott et al., 2020; Koren et al., 2012). Pacific Biosciences (PacBio) initially delivered long yet error-prone reads (initially with a raw base

accuracy of 82.1–84.6%) facilitating short-long read hybrid assembly and long-read-only assembly approaches (Berlin et al., 2015; Koren et al., 2012). Whilst this was also rapidly adopted in the field of plant genomics (Vanburen et al., 2015; Zapata et al., 2016), the application of Nanopore sequencing developed by Oxford Nanopore Technologies (ONT) led to long read sequencing with minimal capital outlay (Michael et al., 2018; Schmidt et al., 2017). Increases in sequencing yield and improvements in raw

base accuracy, as well as protocol development for DNA extraction (Vaillancourt & Buell, 2019; Vilanova et al., 2020), have facilitated the analysis of crop pangenomes (Alonge et al., 2020; Liu et al., 2020; Qin et al., 2021) and the development of near-complete human and Arabidopsis genome sequences (Naish et al., 2021; Nurk et al., 2021).

The PacBio Sequel II platform now delivers long High Fidelity (HiFi) reads with a low error rate. HiFi reads are a consensus of multiple passes of the same circular DNA molecule, typically with a 10–20-kbp genomic DNA insert, and therefore have a much higher per base accuracy (99.5–99.9%) than the individual passes (85%) (Hon et al., 2020; Vollger et al., 2020). The length and low error rate of HiFi reads means that they span the majority of repeated sequences and can also differentiate between highly similar repeated sequences. Various assembly tools have been developed to harness the characteristics of HiFi reads (Cheng et al., 2021; Nurk et al., 2020). HiFi reads are restricted in length because larger DNA insert sizes are sequenced with a lower number of passes, due to limitations of DNA polymerase processivity. ONT has recently relaunched a form of two-pass consensus sequencing but has largely focused on applying deep learning to improve raw read base accuracy to 97% and new Q20+ chemistry is beginning to deliver the promised 99% accuracy. ONT sequencing does not yet provide a raw base accuracy high enough to use the same assembly tools that are used for HiFi reads, yet can generate reads that are multiple megabases in length that can reliably align to reference genomes (Payne et al., 2019). ONT reads in the 20–200 kbp category can span complex tandem arrays of repeated sequences that litter plant genomes. Therefore, current long read sequencing options are either very high quality reads between the length of 10–20 kbp (HiFi) or considerably longer reads with lower per base accuracy (ONT). Despite the apparently complementary strengths of HiFi and ONT data, there have been few attempts to combine the two data types in genome assemblies.

Tomato (*Solanum lycopersicum*) fruits are an important source of vitamins and minerals in a balanced diet and are, globally, the most produced crop in the vegetable category (Costa & Heuvelink, 2018). Tomato varieties can be improved by the introgression of novel resistances to abiotic and biotic stresses from multiple related wild species (Bai & Lindhout, 2007; Foolad et al., 1997; Li et al., 2010; Peralta et al., 2008). High quality reference genomes are available for the cultivated tomato, *S. lycopersicum* cv. 'Heinz 1706' (SL4.0) (Hosmani et al., 2019; Sato et al., 2012), the closely related red-fruited *Solanum pimpinellifolium* 'LA2093' (Wang et al., 2020b), the more distantly related green-fruited *Solanum pennellii* 'LA0716' (Bolger et al., 2014) and the purple/black-fruited *Solanum lycopersicoides* 'LA2951' (Powell et al., 2020). Alongside

these reference genomes, more than 1000 tomato varieties and wild tomato species have been sequenced on Illumina platforms (Aflitos et al., 2014; Gao et al., 2019; Lin et al., 2014) and a panel of 100 of these were recently sequenced using ONT long reads to characterize structural variants (Alonge et al., 2020). In summary, cultivated and wild tomato genomes have been extensively characterized to understand genetic diversity yet even the SL4.0 reference genome contains gaps in repetitive regions, including subtelomeric and centromeric regions.

Tobamoviruses are single stranded RNA viruses that can be devastating pathogens for tomato and other vegetable crops. The tobacco mosaic virus (TMV) and tomato mosaic virus (ToMV) are two tobamoviruses that can infect susceptible tomato cultivars and lead to substantial yield reduction (Lanfermeijer et al., 2003; Lanfermeijer et al., 2005). From the 1930s until the 1960s tomato breeders searched for TMV resistance in various wild tomato species, including *S. pimpinellifolium*, *S. pennellii*, *Solanum habrochaites* (syn. *Lycopersicon hirsutum*), *Solanum chilense* and *S. peruvianum* (Pelham, 1966). TMV resistance was found in *S. pennellii*, *S. habrochaites* (*Tm-1*) and *S. peruvianum* (allelic resistance genes *Tm-2* and *Tm-2²*) (Lanfermeijer et al., 2005; Pelham, 1966). Of the three known TMV resistance genes, introgression of *Tm-2²* from *S. peruvianum* (accession P. I. 128650) has provided dominant, robust and lasting resistance to all TMV and ToMV strains since its discovery in the 1960s and therefore most modern tomato greenhouse varieties contain the *Tm-2²* gene (Alexander, 1963; Schouten et al., 2019). The *Tm-2²* gene encodes a coiled-coil domain Nod-like receptor (CC-NLR) protein that recognizes the movement protein (MP), a key viral protein that facilitates TMV/ToMV movement between plant cells via plasmodesmata (Wang et al., 2020a; Lanfermeijer et al., 2003; Lanfermeijer et al., 2005). The exact size and the structure of the introgression containing the *Tm-2²* gene have remained unknown, although it is known to include at least half of the physical length of chromosome 9 (Lin et al., 2014; Schouten et al., 2019).

Here we sequenced and assembled the genome of the *S. lycopersicum* cultivar Moneyberg-TMV (see Experimental Procedures for breeding history), a popular line used in tomato research because of its vigor, homozygosity and capacity for genetic transformation. PacBio HiFi and ONT Nanopore sequencing reads were independently used to develop highly contiguous genome assemblies. We merged HiFi and ONT assemblies to develop a long-read-only assembly ('MbTMV') where all 12 chromosomes were present as single contigs without the introduction of artificial gaps. The MbTMV assembly was validated through orthogonal approaches including chromosome conformation capture data, mapping of raw long read data and coverage analysis and extensive comparison with the SL4.0 assembly. Through our long-read-only assembly and the

analysis of six commercial tomato hybrids, we show that a minimal 64.1-Mbp introgression has been dragged along with the *Tm-2²* gene despite more than 50 years of tomato breeding.

RESULTS

'Long-read-only' genome assembly, validation and analysis

We generated long read DNA sequences of the *S. lycopersicum* cv. 'Moneyberg-TMV' genome using two different third generation sequencing technologies. High molecular weight (HMW) DNA was extracted and used to construct HiFi sequencing libraries where we made use of two different insert sizes to balance read length and read quality. The two libraries were subjected to PacBio HiFi sequencing on two Sequel II SMRT cells. The first cell yielded 18.8 Gbp with a HiFi read length N50 of 13.9 kbp and a mean quality (*Q*-value) of 28.59 (Table 1). The second cell yielded 21.8 Gbp of data with a HiFi read length N50 of 24.8 kbp and a mean *Q*-value of 24.65 (Table 1). Using the same HMW DNA two identical Nanopore library preparations were performed and subjected to ONT long read sequencing on two PromethION cells. This yielded 100.5 and 101.1 Gbp with respective read length N50 values of 41.6 and 42.4 kbp and mean *Q*-values of 11.28 and 11.18 (Table 1).

We used two genome assembly tools to assemble the HiFi reads and two different tools to assemble the ONT data, and compared the respective outcomes. PacBio HiFi reads were independently assembled using Hifiasm (Cheng et al., 2021) and Canu (Nurk et al., 2020), with respective N50 values of 31.3 and 17 Mbp (Table 2). Both HiFi assemblies contained single contigs that spanned the full length of the SL4.0 reference chromosome 5 (Figure S1). We checked for the completeness of the assembly of gene sequences by Benchmarking Universal Single Copy Orthologs (BUSCO) analysis (Simão et al., 2015) which showed both assemblies were almost gene

complete (both 98.4%), slightly improving upon the SL4.0 genome and comparable to the *S. pimpinellifolium* 'LA2093' genome (Tables 2 and 3). Due to the lower base accuracy of the ONT reads different assembly tools were used in the assembly process. ONT reads were independently assembled using Flye (Kolmogorov et al., 2019) and NECAT (Chen et al., 2021), with respective N50 values of 18.9 and 50.2 Mbp (Table 2). The NECAT assembly contained single contigs that spanned the length of SL4.0 chromosomes 5 and 7 (Figure S1). While the NECAT ONT assembly was more contiguous than either of the HiFi assemblies, gene completeness was lower in both the raw Flye (97.8%) and NECAT (97.1%) assemblies (Table 2), but polishing was able to improve these values. All four assemblies were aligned against the SL4.0 genome and were found to be collinear, irrespective of technology or assembly tool used, except for chromosome 9 where the *S. peruvianum* introgression resides, indicative of mostly correct assemblies (Figure S1).

To test whether sequencing coverage was saturating, we randomly downsampled the HiFi and ONT datasets in intervals of 10% (from 90% down to 10%). Subsequently, we performed nine Hifiasm and nine NECAT assemblies on the respective downsampled datasets (Tables S1 and S2). For Hifiasm, we found that downsampling to as little as 50% (20.3 Gbp; about 24× coverage) of the full HiFi dataset only had a marginal effect on contiguity, indicating that the coverage was saturating (Table S1). For NECAT, which internally selects the longest 40× coverage for assembly, we noticed that downsampling to even just 30% (49.7 Gbp; about 60× coverage) again only had a marginal effect on contiguity. However, care must be taken to avoid NECAT assembly artifacts that occasionally happen even at high coverage (Table S2).

The dot plots of the HiFi and ONT assemblies revealed partial complementarity of the assemblies as the break-points were different (Figure S1 and Dataset S1). To test for complementarity in the assemblies, we designed and implemented an assembly and polishing pipeline that

Table 1 Statistics of different sequencing methods

	PacBio			Oxford Nanopore Technologies		
	Run_1	Run_2	Combined	Run_1	Run_2	Combined
Number of sequences	1 356 407	867 228	2 223 635	4 597 421	4 522 199	9 119 620
Output (Gbp)	18.8	21.8	40.6	100.5	101.1	201.6
Longest read (kbp)	31.3	50.3	50.3	862.3	629.5	862.3
Median read length (kbp)	13.9	24.3	14.7	13.1	13.6	13.4
Mean read length (kbp)	13.9	25.1	18.3	21.9	22.4	22.1
N50 read length (kbp)	13.9	24.8	21.1	41.6	42.4	42.0
Mean quality score	28.59	24.65	26.06	11.28	11.18	11.23

Table 1 shows the total sequencing output and summary statistics for two cells of PacBio HiFi data and two cells of ONT PromethION data, before quality filtering.

Table 2 Statistics of different assembly methods

Input data Assembly	40.6 Gbp (PacBio HiFi)			165.7 Gbp (ONT)		
	Hifiasm	Canu	Hifiasm + Canu	Flye	NECAT	Flye + NECAT
Number of contigs	750	2396	731	371	125	105
Cumulative size (Mbp)	868.9	928.7	871.9	809.7	829.6	829.1
N50 (Mbp)	31.3	17.0	36.8	18.9	50.2	53.4
N90 (Mbp)	8.7	0.08	9.1	5.4	10.6	18.6
L50	10	14	9	15	7	7
L90	32	170	31	45	21	15
Longest contig (Mbp)	66.6	66.7	66.8	47.0	74.2	82.8
BUSCO (genes searched)	5950	5950	5950	5950	5950	5950
BUSCO (complete)	5852	5853	5852	5820	5779	5824
BUSCO (complete) %	98.4	98.4	98.4	97.8	97.1	97.9
BUSCO (complete single)	5739	5735	5739	5703	5666	5713
BUSCO (complete duplicated)	113	118	113	117	113	111
BUSCO (fragmented)	12	12	12	21	38	17
BUSCO (missing)	86	85	86	109	133	109
LAI	13.48	9.65	13.43	10.63	10.39	10.58
Raw LAI	7.85	4.02	7.80	5.00	4.76	4.95

Table 2 shows the summary statistics for assemblies obtained from PacBio and ONT data, respectively. The Flye + NECAT merged assembly presented here does not include polishing of the merged assembly with PacBio data (see Experimental Procedures). BUSCO analysis of the completeness of gene content is based on the Solanales benchmark set.

merged the initial assemblies from the two different sequencing platforms (Figure 1a, Figure S2, Dataset S2 and Experimental Procedures). In the final merged assembly, henceforth referred to as 'MbTMV', 98.9% of the assembly was represented in 12 contigs (N50 = 68.5 Mbp), all with a length of at least 52.2 Mbp, strongly suggestive of a near-complete contig assembly (Table 3). The MbTMV assembly integrated sequences from all four (Hifiasm, Canu, Flye and NECAT) assembly tools (Table S3). Strikingly, when the MbTMV assembly was aligned against the SL4.0 genome assembly the 12 tomato chromosomes were represented as 12 contigs (Figure 1b), as expected from chromosome counting (Figure 1c). In total, 54 contigs making up 8.56 Mbp of sequence were not placed in the 12 major contigs and largely represented chloroplast, mitochondrial, rDNA and satellite repeat derived sequences (Table S4). The unplaced contigs contained just a single complete unique BUSCO gene (of 5950 searched) implicating that the 12 contig assembly is near-complete.

In order to test the structure of the obtained MbTMV assembly we made use of orthogonal approaches. We generated high resolution Omni-C (chromosome conformation capture) data (27.3× coverage) and aligned the paired reads to the MbTMV assembly, and assessed the resulting contact map (see Experimental Procedures). The contact map provided strong support of 12 well-assembled chromosomes, with no changes suggested (Figure 2a). In addition, as validation alone, reference-based (SL4.0) scaffolding of the merged MbTMV assembly was performed, and did not break or improve the assembly (Table S5).

We further checked the assembly by mapping the raw HiFi and ONT reads back to the MbTMV assembly to assess read coverage across the assembly. Indicative of an almost complete assembly, we found mostly even coverage across all 12 chromosomes (Figure 2b; Figure S3), except in a few regions that are notoriously difficult to assemble. Higher ONT coverage was found on chromosomes 1 and 2 overlapping with the highly repetitive 5S rDNA and 45S rDNA regions, respectively (Figure 2b, Figures S3 and S4) (Chang et al., 2008; Perry & Palukaitis, 1990; Schmidt-Puchta et al., 1989; Zhong et al., 1998). A peak of HiFi and ONT coverage on chromosome 11 corresponded to a partial insertion of the mitochondrial genome, that has also been reported in the SL2.50 and SL4.0 assemblies (Figure 2b and Figure S3) (Hosmani et al., 2019; Kim & Lee, 2018). Lower than average HiFi and ONT coverage was found adjacent to centromeric TGR4-dense regions on chromosomes 6, 8 and 11, likely due to difficulties in assembling tandem arrays of 45S rDNA derived satellite repeats that are known to occur in three clusters in the tomato genome (Figure 2b) (Jo et al., 2009). However, other complete chromosomes (including 3, 5, 7, 9 and 10) had very stable coverage even over centromeric regions, indicating near-complete assemblies (Figure 2b and Figure S3). Further to this, we were able to find clusters of TGR1 in all subtelomeric regions apart from one end of chromosome 1 and both ends of chromosome 2, reflecting published FISH results (Figure 2b) (Zhong et al., 1998). We also found long tandem arrays of the telomeric repeat ((TTTAGGG)_n) on 14 of the 24 chromosome ends (Figure 2b) (Ganal et al., 1991).

Table 3 Statistics of different assemblies

Assembly name	MbTMV	SL4.0	LA2093	LA0716
PacBio assembly	HiFiasm v0.14.2; Canu v2.1.1	Canu v1.5	Canu v1.7.1	—
ONT assembly	NECAT; Flye	—	—	—
Polishing	Medaka (ONT); Racon (HiFi)	PacBio + Illumina	PacBio + Illumina	Illumina
Scaffolding	—	Hi-C	Hi-C	Genetic map
Number of sequences	13	13	13	13
Sequences >50 Mbp	12	11	11	13
Cumulative size (Mbp)	833.0	782.5	810.5	989.5
N50 (Mbp)	68.5	65.3	67.2	78
N90 (Mbp)	54.7	53.5	55.6	60.7
L50	6	6	6	6
L90	11	11	11	12
Maximum contig size (Mbp)	96.5	90.9	95.5	109.3
Ns per 100 kbp	0.64	5.72	357.21	11533.09
BUSCO (genes searched)	5950	5950	5950	5950
BUSCO (complete)	5853	5825	5854	5847
BUSCO (complete) %	98.4	97.8	98.4	98.3
BUSCO (complete single)	5743	5718	5744	5711
BUSCO (complete duplicated)	110	107	110	136
BUSCO (fragmented)	12	24	11	17
BUSCO (missing)	85	101	85	86
LAI	13.43	10.39	13.18	7.70
Raw LAI	7.80	4.76	7.55	2.07

Table 3 shows the summary statistics for the MbTMV assembly and three ‘golden standard’ tomato species genome assemblies: *S. lycopersicum* cv. ‘Heinz 1706’ SL4.0 assembly (Hosmani et al., 2019), *S. pimpinellifolium* ‘LA2093’ (Wang et al., 2020b) and *S. pennellii* ‘LA0716’ (Bolger et al., 2014). BUSCO analysis of the completeness of gene content is based on the Solanales benchmark set.

Next, we assessed how the different sequencing technologies and assembly tools complement one another and make scaffolding obsolete. The merged assembly had sequence contributed from all four assembly tools (Table S3), yet the polishing of ONT assemblies by all ONT and HiFi data (see Experimental Procedures) ensured no drop in BUSCO completeness in the final merged sequence compared to raw HiFi assemblies (Tables 2 and 3). In multiple cases where Hifiasm and Canu HiFi assemblies broke, ONT assemblies contained a multi-kilobase AT-rich sequence that was covered by even ONT read coverage, while HiFi read coverage steeply dropped in these regions (Figure S5a–c). An additional multi-kilobase CT/GA simple sequence repeat assembled from ONT reads (and with even ONT read coverage) was not assembled by Hifiasm and Canu, again due to a steep drop in HiFi read coverage (Figure S5d). Opposite to the previous examples, a NECAT assembly breakpoint was assembled from, and evenly covered by, HiFi reads (Figure S5e), further demonstrating the two sequencing technologies can be complementary.

To further assess the MbTMV assembly, we performed in-depth analysis of the MbTMV genome structure and repeat content. We aligned MbTMV with SL4.0 and identified syntenic regions, SNPs, insertions, deletions and other structural variations such as duplications, translocations and inversions (Figure 2d and Dataset S3). Highly increased variation is observed on chromosome 9, where

the *S. peruvianum* introgression is located, with a series of large inversions and extended non-syntenic regions (Figure 2d and Dataset S3). All other chromosomes were highly syntenic between the MbTMV assembly and SL4.0, except for a number of duplications that were identified (Figure 2d). Strikingly, Hifiasm (HiFi), Canu (HiFi) and NECAT (ONT) all led to near-identical assemblies of tandemly repeated sequences in the TGR4-dense centromere of chromosome 5, which was also represented in the final MbTMV merged assembly, adding confidence that the centromere had been spanned in full (Figure 2e, Figure 2f and Figure S6). Finally, chromosome lengths were compared with three ‘golden standard’ tomato species genomes (Figure 2c). MbTMV had slightly longer chromosomes than the SL4.0 and *S. pimpinellifolium* ‘LA2093’ genomes in all cases except for chromosome 2. We suspected this could be related to a better assembly of repeat content, including the subtelomeres and telomeres, but also long terminal repeat (LTR) transposable elements. Consistent with this, we found that the MbTMV assembly had the highest LTR assembly index (LAI) value (Table 3) (Ou et al., 2018). The MbTMV chromosome 9, containing the introgression, was roughly 15.25 Mb longer than that from SL4.0 and similar in size to that from *S. pennellii* ‘LA0716’ (Figure 2c). In summary, the MbTMV genome sequence represents a near-complete assembly of all tomato genes and nuclear chromosomes.

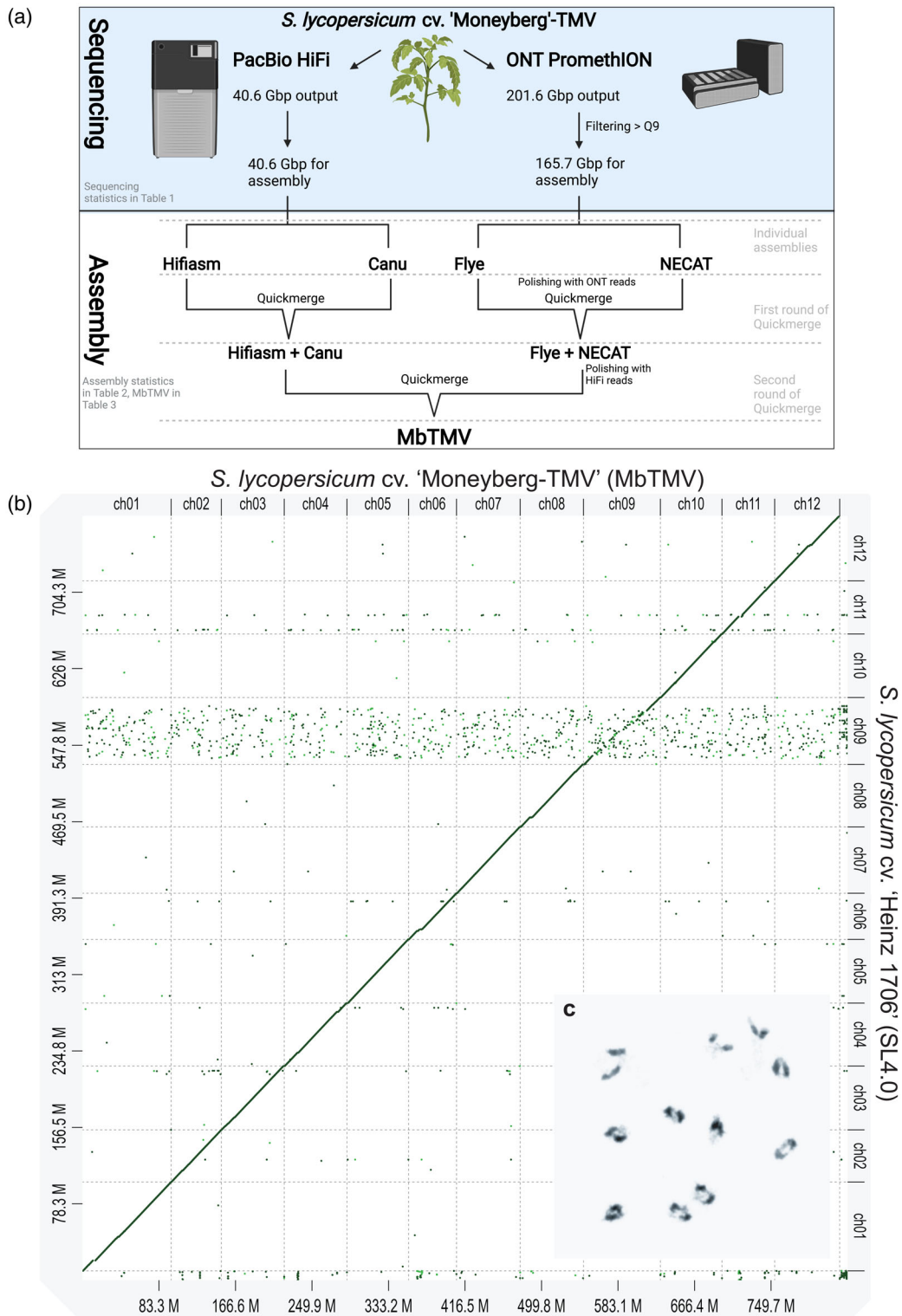


Figure 1. A 'long-read-only' assembly of the tomato genome. (a) Workflow schematic of the MbTMV assembly by merging individual and complementary assemblies from PacBio HiFi and ONT sequencing data. Created with BioRender.com. (b) D-GENIES alignment of the MbTMV assembly against the SL4.0 assembly. Chromosome names were shortened to 'ch01-ch12' for convenience, min identity (abs) was set to 0.65. All chromosomes show near-perfect alignment except for ch09. The x-axis represents the position on the MbTMV genome, where M is megabase pairs. (c) The 12 chromosomes of Moneyberg-TMV paired at diakinesis of the first meiotic division.

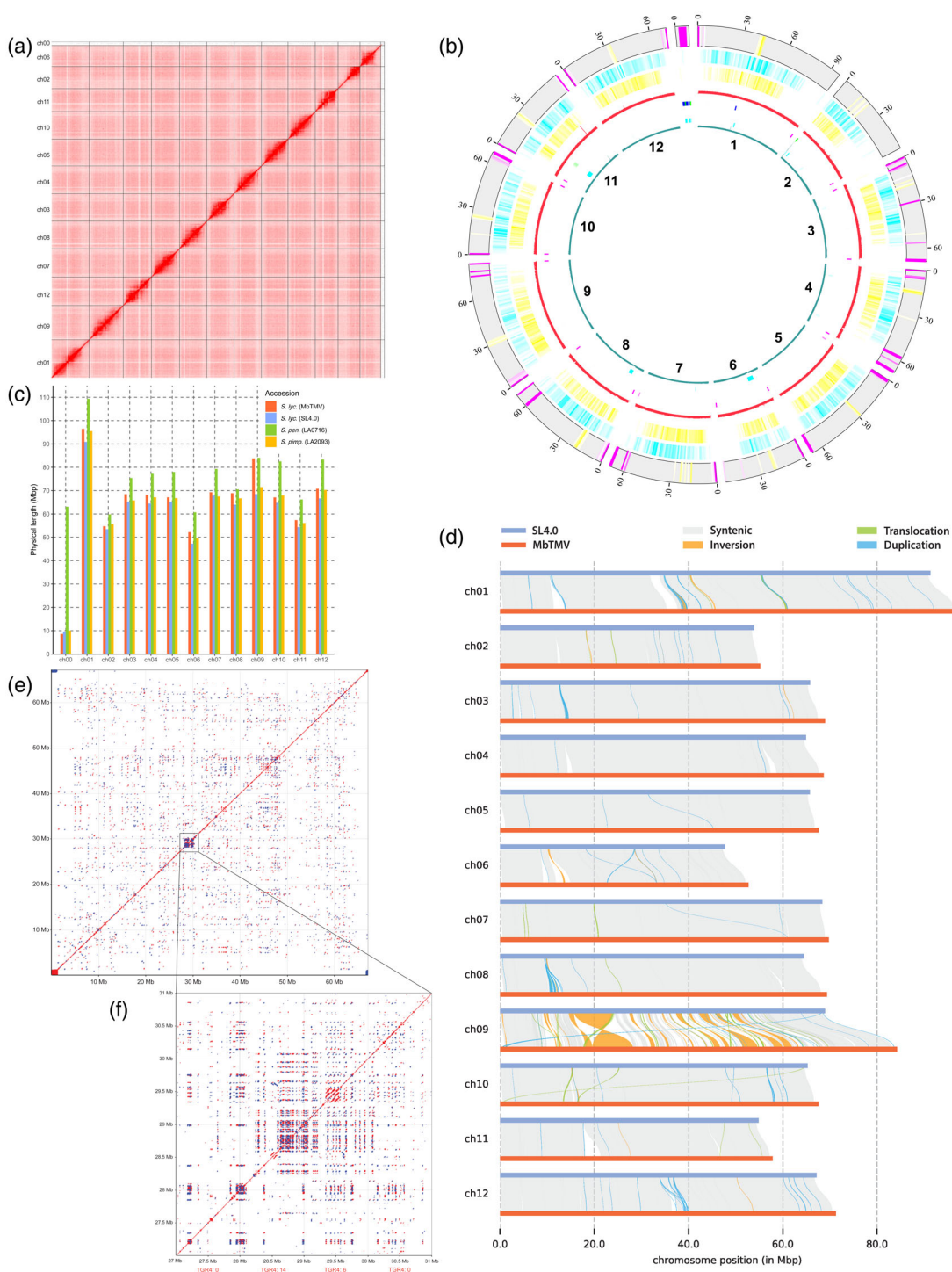


Figure 2. Validation of MbTMV assembly.

(a) Omni-C interaction plot (Hi-C plot as plotted by Juicebox) demonstrating strong interactions within each chromosome of MbTMV. (b) Circos plot of the MbTMV assembly including coverage of raw reads and location of genomic elements. From inner to outer ring: Ring 1 - ONT read coverage (cyan); Ring 2 - 45S rDNA intergenic spacer (IGS) (light blue); Ring 3 - telomeric repeat (pink), 5S rDNA sequence (dark blue), 45S rDNA (light green); Ring 4 - PacBio HiFi read coverage (red); Ring 5 - TGR3 (yellow); Ring 6 - TGR2 (light blue); Ring 7 - TGR1 (pink), TGR4 centromeric repeat (yellow). (c) Chromosome lengths plot of MbTMV assembly and previously published assemblies: *S. lycopersicum* cv. 'Heinz 1706' SL4.0 as, *S. pennellii* 'LA0716' and *S. pimpinellifolium* 'LA2093'. (d) Synteny and rearrangement (SyRI) plot of all 12 MbTMV chromosomes (Query) against all 12 SL4.0 chromosomes (Ref). All chromosomes show high synteny except for chromosome 9. Non-syntenic (non-matching) regions are shown as white gaps between Ref and Query. (e) Self alignment and dot plot analysis of the full length of MbTMV chromosome 5. (f) Self alignment and dot plot analysis of a 4-Mb region of MbTMV chromosome 5 containing the centromere, including identified TGR4 copies (orange), in 1-Mb windows.

In-depth analysis of an alien introgression from *S. peruvianum*

The *Tm-2²* gene confers broad resistance to TMV and ToMV and is located within a large introgression from *S. peruvianum* on chromosome 9, yet the full sequence and structure of the region are not known (Lin et al., 2014). We realigned chromosome 9 sequences from MbTMV and SL4.0, called variants and used polymorphism density to map the exact break points of the introgression. This revealed that the introgression from *S. peruvianum* is 64.1 Mbp (Figure 3a, Figure S7 and Dataset S4). The *S. peruvianum* sequence contains several large inversions compared to SL4.0, but the *Tm-2²* gene is located within a syntenic region (Figure 3a). To better understand the local context of the *Tm-2²* gene in the fully assembled chromosome, we performed further alignments between MbTMV and SL4.0 sequences from approximately 10-Mbp and approximately 1-Mbp regions centered upon the *Tm-2²* gene (Figure 3b,c). Immediately at the start of the introgression, a drop in synteny is observed due to a series of insertions in the *S. peruvianum* derived sequence, followed by several large insertions and deletions and two large inversions (Figure 3b and Dataset S5). At the local scale, the *Tm-2²* gene is located within a syntenic region of about 150.5 kbp that is immediately adjacent to a non-syntenic region that is estimated to be 101.7 kbp longer in *S. peruvianum* (Figure 3c and Dataset S6). We validated our chromosome 9 assembly by aligning ONT reads from a different inbred variety (LYC 1969) that contains the *Tm-2²* gene and a variety that does not (M82), and only found even coverage along chromosome 9 with the LYC 1969 sample, as expected (Figure S8) (Alonge et al., 2020). Further to this, we aligned unassembled short DNA sequences from two other greenhouse tomato cultivars harboring the *Tm-2²* gene, Moneymaker-TMV (MmTMV) and Merlice, with SL4.0. We found that the MmTMV introgression appears to be identical to that found in our MbTMV assembly, whereas the Merlice introgression is estimated to be at least 2.67 Mbp longer (Figure 3d and Figure S7).

Genotyping and haplotyping the alien introgression in modern tomato hybrids

The *Tm-2²* gene is present in the majority of modern tomato greenhouse cultivars; therefore, we set out to check the size of the introgression in five commercial hybrids that were generated in three different breeding programs (Figure 4a,b, Figure S9). To this end we used our assembly to design two polymorphic markers: one at the upstream extreme of the introgression (M-1) and a second at the downstream extreme of the introgression (M-2) (Figure 3a). Using a published marker within the *Tm-2²* gene (M-TM2², Figure 3a), we found that all five hybrids contained the *Tm-2²* gene, two in the heterozygous state (both

produced by Syngenta), whereas the other three were homozygous (Figure 4a,b and Figure S9). The two hybrids heterozygous for the M-TM2² marker were also heterozygous at M-1 and M-2, while the other three hybrids were homozygous at M-1 and M-2 (Figure 4b and Figure S9). The absolute genetic linkage of the three markers in three different, and heavily resourced, tomato breeding programs confirms that conventional backcross breeding has been unable to break down the introgression.

In order to validate the marker genotyping at the chromosome scale, we haplotyped the alien introgression in one of the hemizygous commercial hybrids (*S. lycopersicum* cv. 'Funtelle') using ONT long reads. HMW DNA from the Funtelle hybrid was extracted, and then ONT long reads were generated and assembled using Flye (Figure 4c). The raw assembled contigs were aligned to the MbTMV and SL4.0 sequences and used to extract all contigs aligning to the respective chromosome 9 sequences (Figure 4c). When these contig sequences were competitively realigned to the MbTMV and SL4.0 chromosome 9 sequences (Figure 4c) we found both haplotypes were almost completely covered (Figure 4d). Together, the marker studies (Figure 4b and Figure S9) and analysis of the assembled ONT sequences (Figure 4d) demonstrate that the full introgression is present in a heterozygous state and that ONT reads can discriminate between related haplotypes in hybrid plants.

DISCUSSION

Here, we have assembled a tomato genome *de novo* to chromosome level contigs using long read DNA sequences alone. The raw HiFi and ONT assemblies were highly contiguous and had different breakpoints in the respective assemblies; therefore, merging the assemblies led to further increases in contiguity. Our merged assembly compares favorably (using BUSCO, LAI and chromosome length metrics) with previous tomato genome assemblies that relied on reference- or Hi-C-based scaffolding (Hosmani et al., 2019; Wang et al., 2020b; Bolger et al., 2014; Schmidt et al., 2017; Alonge et al., 2020; Alonge et al., 2019). We made use of the merged assembly to explore the fully assembled 64.1 Mbp introgression from *S. peruvianum* where the *Tm-2²* gene, conferring resistance to ToMV and TMV, resides.

Multiple technical developments have facilitated this highly contiguous tomato genome assembly. Firstly, HiFi reads are highly accurate and downsampling revealed that for inbred tomato as low as 20.3 Gbp (equal to about 24× coverage of our final merged assembly) was sufficient for an assembly with an N50 of 20.8 Mbp, with a largest contig of 66.3 Mbp (Table S1). Secondly, HMW DNA extraction coupled with Circulomics long read enrichment can now reliably lead to ONT PromethION yields of at least 80 Gbp of usable data, with mean read lengths of at least 20 kbp.

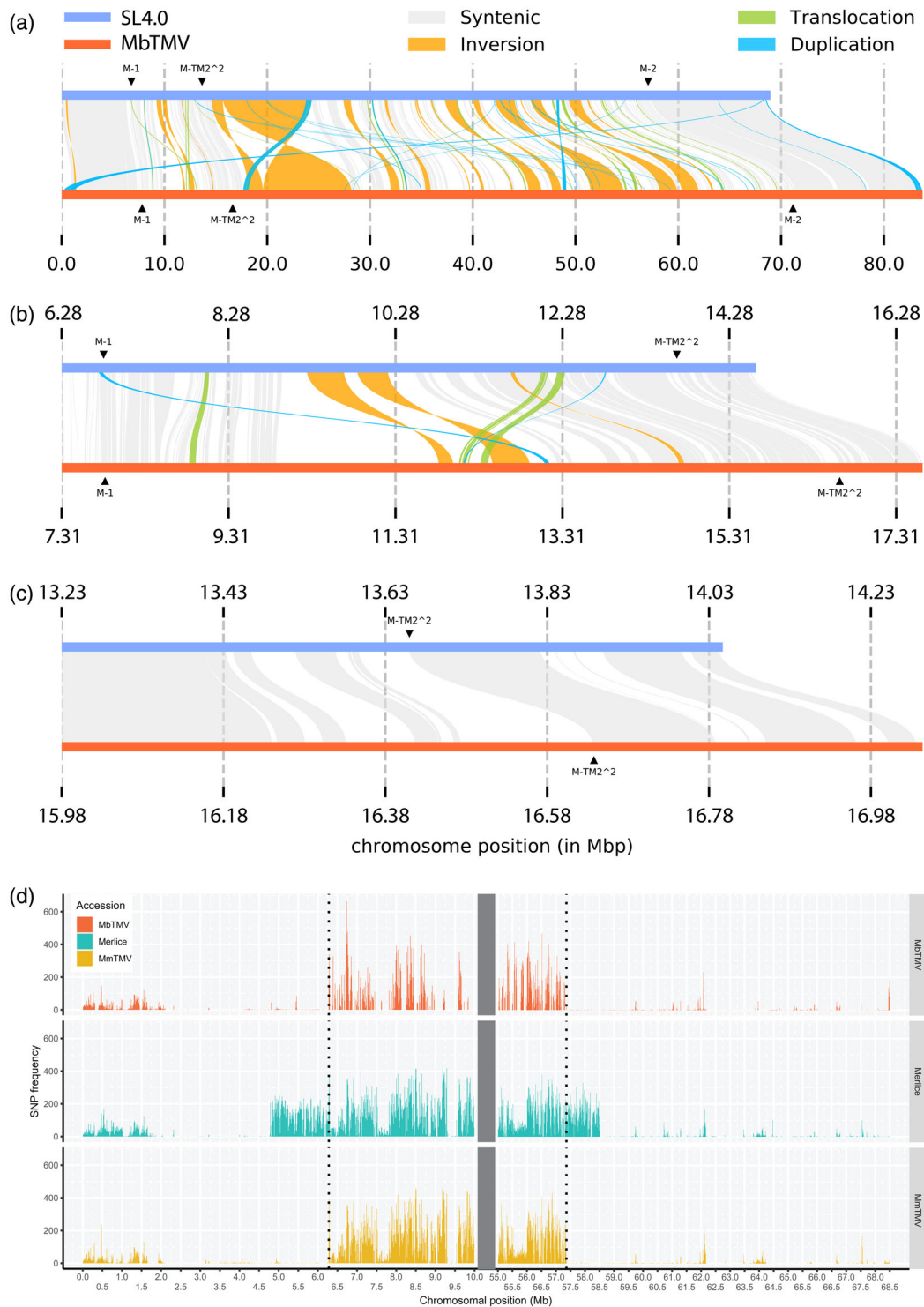


Figure 3. Linkage drag of *S. peruvianum* derived sequence on chromosome 9.

(a) Synteny and rearrangement (SyRI) plot of MbTMV chromosome 9 (Query) aligned against SL4.0 chromosome 9 (Ref). (b) SyRI plot of an approximately 10-Mbp region including the TMV resistance gene locus. (c) SyRI plot of an approximately 1-Mbp region including the TMV resistance gene locus. For (a), (b) and (c), realignments were performed on the specific regions and genomic positions (in Mb) are indicated on SL4.0 (Ref) and MbTMV (Query). M-1, M-TM2² and M-2 indicate genetic markers used in Figure 4(b). Non-syntenic (non-matching) regions are shown as white gaps between Ref and Query. (d) MbTMV, MmTMV (MoneyMaker-TMV) and Merlice variant calling against SL4.0. SNP frequency (calculated in a 10-kbp window) plotted over the first 10 Mbp and the last 13.5 Mbp of SL4.0 chromosome 9. *Solanum peruvianum* introgression was identified by increased SNP frequency. The two dotted vertical lines indicate introgression start and endpoints for MbTMV and MmTMV.

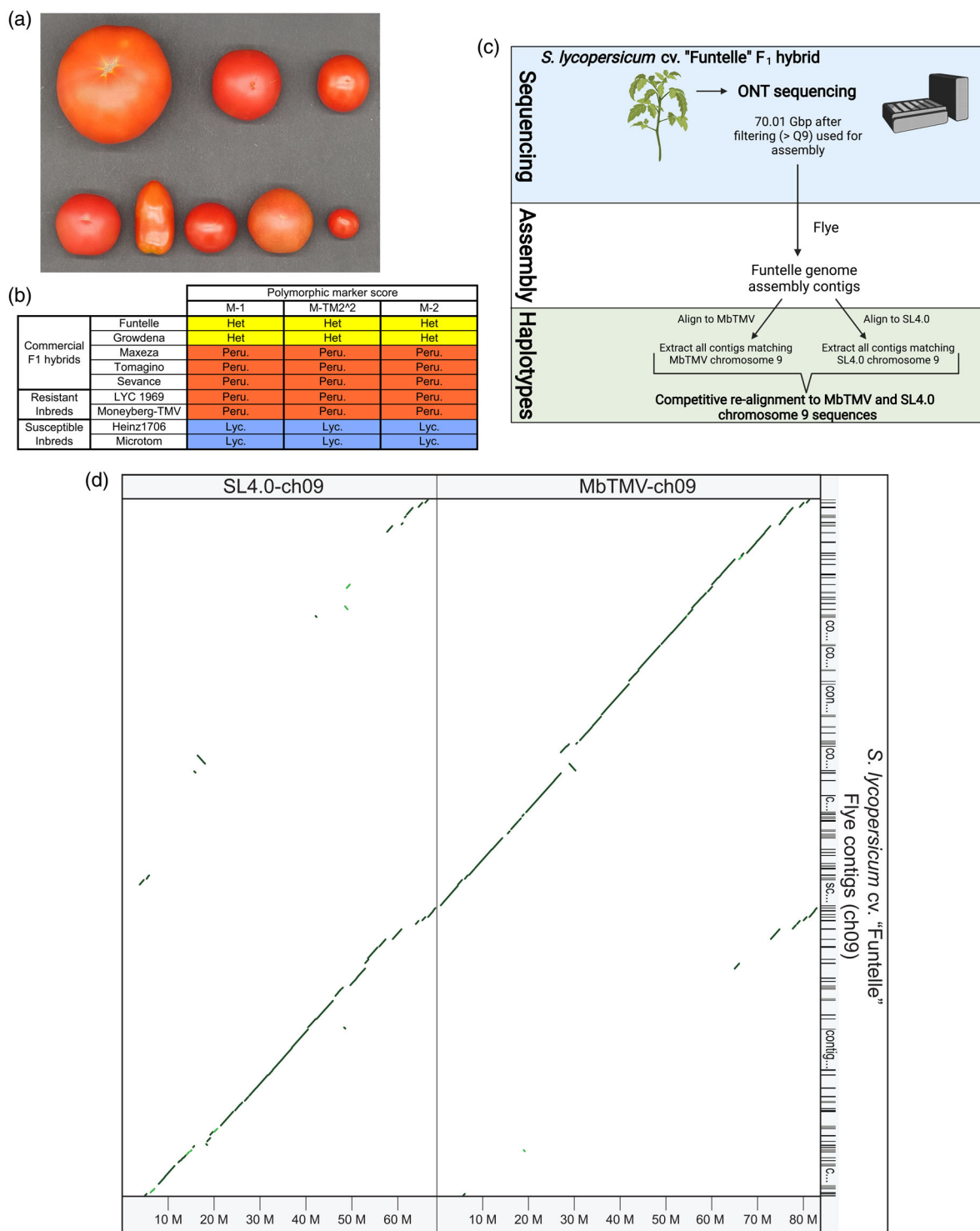


Figure 4. Genotyping and haplotyping-by-sequencing of the TM2² gene introgression in commercial tomato hybrids. (a) Fruit phenotypes of tomato varieties used in this study. Top row, from left: Growdena, Maxeza, Tomagino. Bottom row, from left: Sevance, Funtelle, Moneyberg-TMV × Microtom F1 hybrid, Moneyberg-TMV, Microtom. (b) Marker studies on the TMV resistance introgression from *S. peruvianum* including five commercial hybrids: Maxeza (Truss tomato), Tomagino (Cherry tomato), Funtelle (Date tomato), Growdena (Beefsteak tomato) and Sevance ('on the vine' tomato), two inbred lines resistant to TMV (LYC1969 and Moneyberg-TMV) and two inbred lines susceptible to TMV (Heinz 1706 and Microtom). Marker locations of markers M-1, M-TM2² and M-2 are shown in Figure 3(a). (c) Workflow schematic of Funtelle Flye assembly and the analysis of both chromosome 9 haplotypes. Created with BioRender.com. (d) D-GENIES plot of the Funtelle Flye assembly contigs (right), competitively aligned against both SL4.0 chromosome 9 (top left) and MbTMV chromosome 9 (top right). Min identity (abs) was set to 0.65 and small matches were completely filtered out.

The longer ONT reads can facilitate assemblies with more complete chromosomes (Figure S1), yet gene completeness was slightly lower likely due to higher remaining uncorrectable base errors (Table 2). Thirdly, both HiFi and ONT assembly tools are now computationally efficient and allow the testing of various parameters and input datasets. Our HiFi data was assembled by Hifiasm in less than 2 h with 128 threads, while Flye offers a fast but not as contiguous choice for the ONT platform. Even when using the NECAT assembler, it only takes 3 days with 256 threads to assemble a tomato genome. Finally, by merging the HiFi and ONT assemblies, which had different breakpoints, we were able to harness the complementarity of the two technologies. A recent comparison pointed out that PacBio HiFi reads tend to lead to better assembly of the barley (*Hordeum vulgare*) genome than ONT (Mascher et al., 2021), while here we showed how the complementarity of the two platforms can be leveraged. Highly accurate HiFi reads and the longer, less accurate ONT reads facilitated an assembly that spans many complex repeated sequences. For instance, PacBio HiFi read coverage dropped rapidly at several AT-rich sequences which was complemented by ONT reads and ONT assembly tools (Figure S5a–c). The reduced coverage is potentially due to a ‘heat kill’ step, in which AT-rich sequences may be particularly sensitive to due to annealing properties, during HiFi library preparation (to destroy ligase enzyme) and is no longer recommended in the latest protocols. Here, we also found lower HiFi coverage in a CT/GA-rich region (Figure S5d), as has also been reported in the human genome (Nurk et al., 2021), and its source remains to be identified. As in recent human, Arabidopsis and banana (*Musa acuminata*) genome assemblies (Belser et al., 2021; Naish et al., 2021; Nurk et al., 2021), the 5S rDNA and 45S rDNA sequences were not complete in our assembly, while some tomato centromeres and telomeres appear to be complete, including a convincing telomere-to-telomere (Hifiasm) assembly of chromosome 5 (Figure S6). Both technologies yielded assemblies that would have been impossible just two years ago, and it appears likely that higher quality ONT long read data (through new pore types and basecalling approaches) and longer HiFi reads (through new polymerase types) will further improve assembly metrics in the future. The approach we have used here may be used as a simple recipe in other similar sized, homozygous genomes.

The *Tm-2²* gene is known to be within a large introgression (Lin et al., 2014) but the complete structure of the region has until now remained unassembled. Despite almost six decades of breeding and passing through likely hundreds of backcrosses, there remains absolute linkage between the *Tm-2²* gene and the two extremes of the introgression – a classic case of linkage drag (Figure 4b,d) (Lin et al., 2014; Pelham, 1966; Schouten et al., 2019). The

introgression in Moneyberg-TMV and MmTMV is exactly the same length, agreeing with primary accounts of introgression history (see Experimental Procedures), while the commercial hybrid Merlice, surprisingly, has a slightly longer introgression (Figure 3d). The introgression contains several large inversions but the *Tm-2²* gene itself is found in a region syntenic to *S. lycopersicum* (Figure 3a–c). Pericentromeric heterochromatin makes up about 70% of the tomato genome and meiotic crossovers rarely occur within these regions (De Haas et al., 2017; Demirci et al., 2017; Lhuissier et al., 2007). The *Tm-2²* gene is located within the pericentromeric heterochromatin and that region does not recombine in a Moneymaker × *S. pimpinellifolium* recombinant inbred line (RIL) population (where no *Tm-2²* gene introgression is present), suggesting that the *Tm-2²* gene position on chromosome 9 predisposes it to linkage drag. However, in the same RIL population crossovers do occur up to approximately 1.9 Mbp proximal of the start of the introgression (De Haas et al., 2017). This suggests that the higher polymorphism rate and structural variation between *S. lycopersicum* and *S. peruvianum* (compared to the more closely related *S. lycopersicum* and *S. pimpinellifolium*) likely partially explain the extreme linkage drag in this region.

Why do meiotic crossovers not occur within regions of the introgression that are syntenic to *S. lycopersicum*? It remains to be determined whether meiotic DNA double strand breaks (DSBs), a prerequisite for crossovers, occur within the introgression and whether in hybrids that are hemizygous for the introgression chromosome 9 can completely synapse. Given that the introgression contains many genes and gene promoters/terminators are targets for meiotic DSBs in plants (Choi et al., 2018) it is probable that meiotic DSBs do occur within the introgression region, even in hemizygous hybrids. DSBs inside the introgression are likely repaired as non-crossovers. It is possible that the modulation of factors that can change chromosomal distributions of meiotic crossover (e.g., non-CG DNA methylation) could open up this region to meiotic recombination (Underwood et al., 2018; Wang et al., 2021; Zhao et al., 2021).

Introgression of resistance genes from wild crop relatives can have negative side effects, such as reduced yield and quality, due to linkage drag (Chitwood-Brown et al., 2021; Rubio et al., 2016; Tanksley et al., 1998). Employing the *Tm-2²* gene introgression in a hemizygous state leads to a higher yield in field tomatoes (Tanksley et al., 1998). However, marker studies and ONT-based comprehensive haplotyping showed that only two of the six commercial hybrids we studied employ the introgression in a hemizygous state (Figure 4b,d) (Schouten et al., 2019), which may be due to smaller yield gains of a hemizygous introgression in greenhouse varieties or to reduce the risk of ToMV/TMV infection during the production of hybrid seeds. Nonetheless, the *Tm-2²* gene

introgression from *S. peruvianum* alters the levels of more than 300 metabolites (Zhu et al., 2018), suggesting factors linked to the *Tm-2²* gene compromise multiple important tomato traits. We expect that the rapid generation of near-complete genome assemblies will be exploited in the future to decode additional introgressions from wild crop relatives, and subsequent genome engineering will lead to resistant crop varieties with better yield and taste.

EXPERIMENTAL PROCEDURES

Plant materials and growth

Moneyberg-TMV was originally developed at De Ruiter seeds (Bleiswijk, Netherlands) by introgression of the *Tm-2²* gene from a source that contained *S. peruvianum* germplasm originally provided by Alexander (Alexander, 1963). The *S. lycopersicum* basis of the line originates from the Moneyberg cultivar, an open pollinated, indeterminate greenhouse tomato cultivar that was developed by selection from Moneymaker at Van den Berg seeds (Gebr. van den Berg, Naaldwijk, Netherlands). Moneymaker itself was first developed in the early 1900s by Fred Stonor (Southampton, England, UK). Maxeza F1 (Truss tomato) and Tomagino F1 (Cherry tomato) were produced by Enza Zaden. Funtelle F1 (Date tomato) and Growdena F1 (Beefsteak tomato) were produced by Syngenta. Sevance F1 ('on the vine' tomato) and Merlice F1 (Truss tomato) were produced by De Ruiter seeds. MmTMV seeds were from the stocks of Wageningen University & Research (WUR)-Plant breeding which were originally provided by De Ruiter seeds. For further seed origin information please see the acknowledgments.

For genome sequencing and meiotic cytology, 10 Moneyberg-TMV plants (all progeny of a single highly inbred parent) were grown in the MPIPZ greenhouses during the late spring of 2020 under natural light supplemented with artificial light to ensure 16 h light per day. Young unexpanded leaves were collected from 5-week-old plants and snap frozen in liquid nitrogen before interim storage at -80°C . For whole genome resequencing, MmTMV and Merlice plants were grown in the greenhouses of WUR until the third full leaf, and shoot tips with young leaves were harvested and snap frozen in liquid nitrogen. For marker studies, Moneyberg-TMV, LYC1969, Microtom, Heinz 1706, Maxeza, Tomagino, Funtelle, Growdena and Sevance seeds were germinated *in vitro* on 0.8% agarose.

Chromosome spreading

Appropriate stages (3–4 mm) of meiotic buds from Moneyberg-TMV were fixed in 1 ml fresh Carnoy's solution composed of 3:1 (v/v) absolute ethanol:glacial acetic acid and placed under vacuum for at least 30 min to ensure tissue infiltration. The Carnoy's solution was replaced and the samples were kept at room temperature for 48 h until they turned white. The fixed materials were used for chromosome spreading essentially as previously described (Ross et al., 1996). In brief, 50–60 meiotic anthers were isolated from meiotic buds and placed into a 50- μl enzyme mixture (0.3% cellulase, 0.3% cytohelicase and 0.3% pectolyase in 10 mM citric buffer, pH 4.6) to digest for 2.5 h at 37°C . Two to three anthers were used to make a single slide. After drying 8 μl DAPI (2 $\mu\text{g ml}^{-1}$) was added to stain the chromosomes. Finally, meiocytes images were taken using a Zeiss Axio Imager Z2 Microscope and images were analyzed using Zeiss ZEN 2 (blue edition) software.

Moneyberg-TMV high molecular weight DNA extraction

HMW DNA of Moneyberg-TMV was isolated from 1.5 g of young leaf material with a NucleoBond HMW DNA kit (Macherey Nagel, Düren, Germany). DNA quality was assessed with a FEMTOpulse device (Agilent, Santa Clara, CA, USA) and quantity was measured using a Quantus Fluorometer (Promega, Madison, WI, USA).

Moneyberg-TMV library preparations and sequencing

A HiFi library was prepared according to the manual 'Procedure & Checklist - Preparing HiFi SMRTbell® Libraries using SMRTbell Express Template Prep Kit 2.0' with an initial DNA fragmentation by g-Tubes (Covaris, Woburn, MA, USA) and final library size binning into defined fractions by SageELF (Sage Science, Beverly, MA, USA). Size distribution was again controlled by FEMTOpulse (Agilent). Size-selected libraries with an expected insert size of 15 and 18 kbp were independently sequenced on single SMRT cells of a Pacific Biosciences Sequel II device at MPG Cologne with Binding kit 2.0 and Sequel II Sequencing Kit 2.0 for 30 h (Pacific Biosciences, Menlo Park, CA, USA).

Nine micrograms of HMW DNA was size-selected using the Circulomics Short-Read Eliminator XL Kit (Circulomics Cat# SKU SS-100-111-01). Out of this size-selected DNA 1.5 μg was used as input for two library preparations with the Oxford Nanopore LSK-110 ligation sequencing Kit. Half of each library was loaded onto a PromethION FLO-PRO002 flowcell (R9.4.1 pores) and sequenced for 24 h. Then the flowcells were rinsed using the Oxford Nanopore Wash Kit WSH-003 and the second part of each library was loaded and sequencing continued for another 48 h. ONT sequencing was performed on an Oxford Nanopore P24 PromethION at the Forschungszentrum Jülich using MinKNOW version 21.02.7 without live basecalling. Basecalling of the Oxford Nanopore read data was done using guppy basecaller version 5.0.11 using the R9.4.1 PromethION superhigh accuracy model (dna_r9.4.1_450bps_sup_prom) including filtering out basecalled reads with an average Phred-Score of less than 9.0. Reads with a Q-value below 9 were excluded before further analysis, including genome assembly. To remove adapter sequences and split chimeric reads the remaining Nanopore reads were then filtered further with porechop version 0.2.4 with default settings.

A chromatin conformation capture library was prepared using 0.5 g of young leaf material as the input. All treatments were according to the recommendations of the kit vendor (Omni-C, Dovetail) for plants. As a final step, an Illumina-compatible library was prepared (Dovetail) with an insert size of 540 bp and sequenced (paired end 2 \times 150 bp) on an Illumina NovaSeq 6000 at Novogene to generate 148.54 million PE reads.

Whole genome resequencing

MmTMV and Merlice plant material was ground into fine powder by mortar and pestle, and DNA was isolated by a CTAB-based method (Healey et al., 2014). DNA was dissolved in ultrapure water and DNA was checked by gel, Qubit and nanodrop. Library preparation and whole genome sequencing were performed by Novogene using an Illumina device.

Genome assemblies and assembly statistics

Hifiasm v0.14.2 (Cheng et al., 2021) was used to assemble the HiFi reads with default settings. Canu v2.1.1 was used to assemble the HiFi reads in 'HiCanu' mode (Nurk et al., 2020) with an estimated genome size of 916 Mbp based on kmer counting of the raw HiFi data using Jellyfish v2.2.6 (Marçais & Kingsford, 2011).

Flye v2.8.2 (Kolmogorov et al., 2019) was used to assemble the ONT reads with the option `--nano-raw` for unpolished Nanopore reads. NECAT version 0.0.1_update20200803 was used to assemble the ONT reads (Chen et al., 2021) with default options apart from increasing the coverage used for assembly from 30× to 40× by setting `PREP_OUTPUT_COVERAGE` to 40.

ONT and HiFi reads were randomly subsampled in nine sets of 90, 80, 70, 60, 50, 40, 30, 20 and 10% of the original reads and used for assemblies using NECAT (ONT) and Hifiasm (HiFi) with the same settings as for the original assemblies.

Quast v5.0.2 (Mikheenko et al., 2018) and GAAS v1.1.0 (<https://github.com/NBISweden/GAAS>) were used to calculate statistics on fasta files. BUSCO was calculated using BUSCO v5.2.1 (Seppey et al., 2019) depending on `hmmsearch` v3.1, and `metaeuk` v4.a0f584d was used with lineage datasets `solanales` (https://busco-data.ezlab.org/v5/data/lineages/solanales_odb10.2020-08-05.tar.gz) and `eudicots` (https://busco-data.ezlab.org/v5/data/lineages/eudicots_odb10.2020-09-10.tar.gz) to obtain evolutionarily informed expectations of gene content. To assess the LAI, LTR retriever v2.9.0 (Ou et al., 2018) was run with default settings on the respective genome assemblies.

MbTMV assembly pipeline

The NECAT assembly was polished with all of the ONT reads using Medaka v1.2.3 (<https://nanoporetech.github.io/medaka/>) and the model specific for PromethION R.9.4.1 data basecalled with guppy 5.0.11 in 'superhigh accuracy' mode. The Flye assembly was also polished as described above.

Next, the NECAT 40x medaka and Flye v2.8.2 medaka assemblies were merged. This was done by running `nucmer` (part of `mummer` v.4.0.0rc1) with the `-l` parameter to prevent invalid contig links using the NECAT assembly as query and the Flye assembly as reference. The alignment table was then filtered with `delta-filter` (also part of `mummer`) using the options `-r -q -i 0.95` to only use reciprocal best matches per region and a minimum identity of 95% in overlaps. This matches the default settings in the `quickmerge` wrapper which still relies on `mummer` version 3. Finally `quickmerge` (Chakraborty et al., 2016) was used with the parameter `-c 7.0` to increase stringency of merging regions to prevent assembly artifacts. The other parameters mandatory for `quickmerge` were set to the same values as used in the wrapper script by default (`-hco 5.0 -l 0 -ml 5000`). The resulting merged assembly was subsequently polished with all HiFi reads using `Racon` v1.4.3 (Vaser et al., 2017) together with `Minimap` version 2.21 (Li, 2018) using the 'map-hifi' preset for mapping the reads to the genome to overcome uncorrectable errors resulting from Nanopore reads.

In parallel, the `Canu` and `Hifiasm` assemblies were merged using the `Canu` assembly as reference and the `Hifiasm` assembly as query with `quickmerge` (as above) but using the default `-c` parameter of 1.5. Due to the low baseline error rate of HiFi Reads no further polishing was done on these assemblies.

The resulting merged (and polished) assemblies were then merged again using the Nanopore (Flye+NECAT) as query and the `PacBio` (`Hifiasm+Canu`) as reference using the same default parameters as for merging the two `PacBio` assemblies before. The final merged assembly was named MbTMV.

Dot plots

D-GENIES version 1.2.0 (Cabannes & Klopp, 2018) was run with default settings with alignments generated using `Minimap2` v2.21 (Li, 2018) providing the *S. lycopersicum* cv. 'Heinz 1706' SL4.0 (Hosmani et al., 2019) as reference (target) and our assembly as

query. For legibility the chromosome names in both assemblies were shortened to 'ch01–ch12'. Local installations of `reDOTable` v1.1 (<https://www.bioinformatics.babraham.ac.uk/projects/redotable/>) or `GitHub` (<https://github.com/s-andrews/redotable>) were used to generate dot plots.

Validation of MbTMV assembly

Following the `esrice/hic-pipeline` (<https://github.com/esrice/hic-pipeline>), `Omni-C` (Dovetail) paired end reads were mapped separately using `Burrows-Wheeler Aligner` v0.7 (Li & Durbin, 2009) and the `filter_chimeras.py` script. Mapped reads were combined using the `combine_ends.py` script, with three iteration steps and a minimum mapping quality value of 20 (default), followed by adding read mate scores, sorting and removing duplicate reads using `Samtools` v1.9 (Danecek et al., 2021). The resulting `bam` file was converted to a `bed` file and sorted (`-k 4`) using `Bedtools` v2.30 (Quinlan & Hall, 2010). We ran one single round of `Salsa` v2.2 (Ghurye et al., 2019) with optional settings: `-e DNASE -m yes -p yes`.

A modified version of the `convert.sh` script was used to convert the `Salsa2` output to a Hi-C file, which was used within a local installation of `Juicebox` (<https://github.com/aidenlab/Juicebox>) v1.11.08 to generate a Hi-C contact plot.

The MbTMV genome assembly was aligned to SL4.0 (Hosmani et al., 2019) using `Minimap2` v2.17 (Li, 2018) with default settings, followed by running `RaGOO` v1.11 (Alonge et al., 2019) with default options.

Coverage analysis and circos plot of MbTMV assembly

ONT data were mapped using `Minimap2` version 2.18-r1028-dirty (Li, 2018) with the preset 'map-ont', whereas `PacBio` HiFi data were mapped with the preset 'map-hifi'. The output `SAM` file was converted, sorted and indexed using `Samtools` v1.9 (Danecek et al., 2021). `Samtools` v1.9 (Danecek et al., 2021) was used to extract the coverage per base, including positions with zero depth, from the `bam` file. The resulting average depth was summarized in overlapping windows of 200 kbp every 100 kbp and visualized using `NG-circos` (Cui et al., 2020). In addition, sequences of the 45S rDNA intergenic spacer, 5S rDNA, 45S rDNA, telomeric repeat and TGR1-4 were searched in MbTMV using `blastn` and counted in non-overlapping windows of size 1 Mbp.

For the coverage plot in Figure S3, `PacBio` HiFi data were mapped to the MbTMV genome assembly using `pbmm2` (version 1.4.0) with the preset 'CCS' (<https://github.com/PacificBiosciences/pbbioconda>). ONT data were mapped to the MbTMV genome using `Minimap2` version 2.17 (Li, 2018) with the preset 'map-ont' and 'eqx', followed by converting, sorting and indexing of the output file using `Samtools` v1.9 (Danecek et al., 2021). Read coverage was extracted in 100-kbp windows using `Mosdepth` (Pedersen & Quinlan, 2018) and plotted in the middle of each interval within `R` version 4.0.3 (2020-10-10) (<https://cran.r-project.org/>) using `ggplot2` and the `tidyverse` package (<https://www.tidyverse.org/>).

For Figure S5, `PacBio` HiFi and ONT-NECAT read coverage was visualized using a local installation of `IGV` (v2.8.13) (Robinson et al., 2011).

Genome alignment, SV detection and further genome analysis

Genomes were aligned to SL4.0 (Hosmani et al., 2019) using `Minimap2` v2.17 (Li, 2018) with options `-ax asm5 --eqx`, followed by running `SyRI` v1.4 (Goel et al., 2019), to identify and call polymorphisms and structural variations, with optional settings: `-k -F S --log`

WARN. Plotsr v5 (Goel et al., 2019) was used with options -B <annotation.bed> -H <1-9> and -W <1-9> to generate SyRI plots. Fasta headers of genomes were manually formatted to match between genomes using the sed command line and chromosome 0 was removed using the awk command line before aligning the genomes. Chromosomes 1, 2, 7, 8 and 12 of the MbTMV assembly were reverse complemented before alignment using the cat command line.

Using the SyRI generated vcf output of the whole chromosome alignment (Dataset S4), sequences used for Figure 3b,c were extracted (SL4.0:6286825–14549782 MbTMV:7314513–17630288 and SL4.0:13227892–14039189 MbTMV:15980168–17044082 for Figure 3b,c, respectively) using Samtools v1.9 (Danecek et al., 2021). Sequences were aligned using Minimap2 v2.17 (Li, 2018) with options -ax asm5 --eqx followed by running SyRI v1.4 and Plotsr v5 (Goel et al., 2019). Figure 3b,c were manually edited using Adobe Illustrator 25.2.3 adding genomic positions based on extracted regions.

Chromosome lengths were extracted from the fasta files, MbTMV, *S. lycopersicum* cv. 'Heinz 1706' SL4.0 (Hosmani et al., 2019), obtained from ftp://ftp.solgenomics.net/genomes/Solanum_lycopersicum/Heinz1706/assembly/build_4.00/S_lycopersicum_chromosomes.4.00.fa, *S. pennellii* 'LA0716' (Bolger et al., 2014), obtained from ftp://ftp.solgenomics.net/genomes/Solanum_pennellii/Spenn.fasta, and *S. pimpinellifolium* 'LA2093' v1.5 (Wang et al., 2020b), obtained from ftp://ftp.solgenomics.net/genomes/Solanum_pimpinellifolium/LA2093/Spimp_LA2093_genome_v1.5/LA2093_genome_v1.5.fa, using the awk command line and plotted within R version 4.0.3 using ggplot2 and the tidyverse package.

Further analysis of chromosome 9 introgression

M82 and LYC 1969 ONT data (Alonge et al., 2020) were mapped to both SL4.0 and MbTMV using Minimap2 v2.17 (Li, 2018), with the options -ax map-ont --eqx. The output SAM file was converted, sorted and indexed using Samtools v1.9 (Danecek et al., 2021). Coverage plots per chromosome were constructed with goleft IndexCov v0.2.4 (Pedersen et al., 2017).

MoneyMaker and Merlice Illumina data were mapped to SL4.0 using bowtie2 v2.2.8 with options -q --phred33 --very-sensitive --no-unal -p 12 -x <SL4.0.fasta> -U reads1.fq,reads2.fq -S. Variant calling was done using bcftools v1.9 mpileup and call with options -mv -Ov (Li, 2011) (<https://samtools.github.io/bcftools/bcftools.html>).

SNP density was extracted from MbTMV (SyRI output), MoneyMakerTMV and Merlice vcf files using VCFtools v.0.1.16 (Danecek et al., 2011). Plots were made within R 4.0.3 (2020-10-10) (<https://cran.r-project.org/>) using ggplot2 and the tidyverse package (<https://www.tidyverse.org/>).

Marker studies

Cotyledons from *in vitro* germinated samples were collected and lyophilized overnight in an Alpha 1-4 freeze dryer (Martin Christ GmbH). DNA extraction was performed using the BioSprint 96 DNA Plant kit (Qiagen) and eluted in 200 µl AE buffer. M-1 was amplified using the primers dCUn0256 (GGAACCTCGAGTCCTTACAGT) and dCUn0257 (GGCAGCCATTAGCAAACCCA). M-TM2^Δ2 was amplified using published primers (Lanfermeijer et al., 2005). M-2 was amplified using the primers dCUn0258 (TTCTGTTCCA-GACCCGACCT) and dCUn0259 (CCATTAACTCCAGACGGG). Thirty-five rounds of PCR were performed using Mango Taq (Bio-line) under standard conditions. M-1 was digested with *Afl*III (NEB) overnight at 37°C, M-TM2^Δ2 was digested with *Bsl*I (NEB) for 3 h at 55°C and M-2 was digested with *Xho*I (NEB) overnight at 37°C. Per restriction digest, 10 µl was loaded on a 3% agarose gel.

Funtelle F₁ hybrid sequencing, genome assembly and analysis

DNA from the hybrid *S. lycopersicum* cv. 'Funtelle' were extracted using the Machery Nagel Nucleobond HMW DNA Kit. HMW DNA was size-selected using the Circulomics Short-Read Eliminator XL Kit (Circulomics Cat# SKU SS-100-111-01) and used as input for library preparation with the Oxford Nanopore LSK-110 ligation sequencing Kit. Four libraries from the same sample were loaded onto three PromethION FLO-PRO002 flowcells and one MinION flowcell (all R9.4.1 pores) and sequenced. ONT sequencing was performed on an Oxford Nanopore P24 PromethION and a MinION MK1B at the Forschungszentrum Jülich using MinKNOW version 21.02.7 without live basecalling. Basecalling of the Oxford Nanopore read data was done using guppy basecaller version 5.0.11 using the R9.4.1 PromethION superhigh accuracy model (dna_r9.4.1_450bps_sup_prom) and the R9.4.1 MinION superhigh accuracy model (dna_r9.4.1_450bps_sup). ONT reads were assembled with Flye v2.8.2 using the same settings as for 'Moneyberg-TMV'. The contigs from the Flye assembly of 'Funtelle' were separately aligned against the MbTMV and SL4.0 assemblies using Minimap2 v2.21 and the alignments were interrogated using D-GENIES version 1.2.0 (default settings). All contigs that aligned to Chr9^{MbTMV} or Chr9^{SL4.0} were extracted and competitively realigned using Minimap2 v2.21 to a fasta file containing both Chr9^{MbTMV} and Chr9^{SL4.0}, and the alignment was visualized using D-GENIES version 1.2.0 (default settings).

ACKNOWLEDGMENTS

Moneyberg-TMV seeds were kindly provided for research purposes by Cilia Lelivelt and Maarten Verlaan (Rijk Zwaan, Netherlands). Maxeza F₁ and Tomagino F₁ tomato seeds were kindly provided for research purposes by Martijn van Stee (Enza Zaden, Netherlands). Funtelle F₁ and Growdena F₁ tomato seeds were kindly provided for research purposes by Axel Voss (Syngenta, Germany). Sevance F₁ seeds (De Ruiter seeds, part of Bayer Group) were purchased for research purposes from Volmary GmbH (Münster, Germany). Merlice F₁ seeds (De Ruiter seeds, part of Bayer Group) were provided by Tomato World (Netherlands) to HJS for research purposes. Microtom seeds were originally sourced from the Tomato Growers Supply company (Ft. Myers, Florida, USA). LYC1969 seeds were a gift from Zachary Lippman (CSHL, USA). Heinz 1706 seeds were provided by the Centre for Genetic Resources (Wageningen, Netherlands). We are grateful to Gerard Bijsterbosch (WUR) for isolating DNA from MmTMV and Merlice. We thank Saurabh Pophaly (MPIPZ), Manish Goel (MPIPZ) and Danny Esselink (WUR) for assistance with bioinformatic analysis. We thank Korbinian Schneeberger (MPIPZ), Quentin Gouil (Walter and Eliza Hall Institute) and Alex Canto-Pastor (UC Davis) for comments on the manuscript. Information on the breeding history of MoneyMaker, Moneyberg and Moneyberg-TMV varieties was kindly provided by Theo Schotte (Solynta, Netherlands) and Maarten Koornneef (WUR/MPIPZ). This work was supported by the Max Planck Society, a PhD fellowship awarded to MWAMZ from the Malaysian Agricultural Research and Development Institute (MARDI), grants awarded to BU (DFG US 98/23, CEPLAS EXC2048 and BMBF 031A536C) and the WUR Department of Plant Breeding (HS). This manuscript is dedicated to Eric Robinson Smith, whose favorite tomato variety was MoneyMaker.

AUTHOR CONTRIBUTIONS

WMJR and SE cultivated and collected plant materials. BH performed DNA extractions and HiFi sequencing. MHWS

and DBL performed DNA extractions and ONT sequencing. MHWS, WMJR and DBL performed genome assemblies. MHWS performed downsampling analysis and assembly merging. WMJR performed validation of the merged assembly and the majority of the downstream bioinformatic analysis with contributions from MHWS. YW performed chromosome spreading experiments. HJS contributed Illumina sequencing data for MmTMV and Merlice. All authors contributed to the analysis and interpretation of data. WMJR generated the main and supplementary figures with contributions from MWHS, BU and CJU. CJU coordinated the project. WMJR, MWHS, BU and CJU wrote the manuscript with comments from all other authors.

CONFLICTS OF INTERESTS

The authors declare that they have no competing interests.

SUPPORTING INFORMATION

Additional Supporting Information may be found in the online version of this article.

Figure S1. Alignment of four Moneyberg-TMV genome assemblies with Heinz 1706 (SL4.0) assembly.

Figure S2. Alignment of the merged assemblies to SL4.0.

Figure S3. PacBio HiFi and ONT coverage plots.

Figure S4. Dot plot of self-alignment of repetitive regions on MbTMV chromosomes 1 and 2.

Figure S5. Examples of complementary sequencing data visualized in IGV.

Figure S6. Synteny plots of different chromosome 5 assemblies.

Figure S7. SNP frequency plot between MbTMV and SL4.0 in 10-kbp windows along chromosome 9.

Figure S8. Coverage plot of LYC1969 and M82 ONT reads aligned to MbTMV chromosome 9 and SL4.0 chromosome 9.

Figure S9. Agarose gel image of molecular marker analysis.

Dataset S1. PAF files showing the approximate mapping positions between SL4.0 and non-merged Moneyberg-TMV assemblies.

Dataset S2. PAF files showing the approximate mapping positions between SL4.0 and merged Moneyberg-TMV assemblies.

Dataset S3. SyRI called variants between MbTMV chromosome 9 and SL4.0 chromosome 9, extracted from the whole genome alignment.

Dataset S4. SyRI called variants between MbTMV chromosome 9 and SL4.0 chromosome 9, from a direct alignment of MbTMV chromosome 9 and SL4.0 chromosome 9.

Dataset S5. SyRI called variants between MbTMV chromosome 9 and SL4.0 chromosome 9, from an approximately 10-Mb extracted region.

Dataset S6. SyRI called variants between MbTMV chromosome 9 and SL4.0 chromosome 9, from an approximately 1-Mb extracted region.

Table S1. Downsampling of PacBio HiFi reads and assembly using Hifiasm.

Table S2. Downsampling of ONT reads and assembly using NECAT.

Table S3. Transition points of the MbTMV assembly.

Table S4. Classification of unplaced contigs in the MbTMV assembly.

Table S5. Statistics of MbTMV assembly and RaGOO output.

OPEN RESEARCH BADGES



This article has earned an Open Data badge for making publicly available the digitally-shareable data necessary to reproduce the reported results.

DATA AVAILABILITY STATEMENT

PacBio HiFi consensus reads (Moneyberg-TMV), ONT sequencing reads (Moneyberg-TMV), Omni-CAUTHOR: Please check "Omni-C" is correct. Illumina reads (Moneyberg-TMV) and the MbTMV genome assembly were deposited in the EMBL-EBI European Nucleotide Archive under project number PRJEB44956. ONT sequencing reads for Funtelle and Illumina reads for MmTMV and Merlice are also deposited under the same accession code. The Flye genome assembly from Funtelle ONT reads is made available at Dryad (<https://doi.org/10.5061/dryad.3j9kd51kn>).

REFERENCES

- Aflitos, S., Schijlen, E., de Jong, H., de Ridder, D., Smit, S., Finkers, R. *et al.* (2014) Exploring genetic variation in the tomato (*Solanum section Lycopersicon*) clade by whole-genome sequencing. *The Plant Journal*, **80**, 136–148.
- Alexander, L.J. (1963) Transfer of a dominant type of resistance to the four known Ohio pathogenic strains of tobacco mosaic virus (TMV) from *Lycopersicon peruvianum* to *L. esculentum*. *Phytopathology*, **53**, 896.
- Alonge, M., Soyk, S., Ramakrishnan, S., Wang, X., Goodwin, S., Sedlazeck, F.J. *et al.* (2019) RaGOO: fast and accurate reference-guided scaffolding of draft genomes. *Genome Biology*, **20**, 224.
- Alonge, M., Wang, X., Benoit, M., Soyk, S., Pereira, L., Zhang, L. *et al.* (2020) Major impacts of widespread structural variation on gene expression and crop improvement in tomato. *Cell*, **182**, 145–161.e23.
- Bai, Y. & Lindhout, P. (2007) Domestication and breeding of tomatoes: What have we gained and what can we gain in the future? *Annals of Botany*, **100**, 1085–1094.
- Belser, C., Baurens, F.-C., Noel, B., Martin, G., Cruaud, C., Istace, B. *et al.* (2021) Telomere-to-telomere gapless chromosomes of banana using nanopore sequencing. *Communications Biology*, **4**, 1047.
- Berlin, K., Koren, S., Chin, C.S., Drake, J.P., Landolin, J.M. & Phillippy, A.M. (2015) Assembling large genomes with single-molecule sequencing and locality-sensitive hashing. *Nature Biotechnology*, **33**, 623–630.
- Bolger, A., Scossa, F., Bolger, M.E., Lanz, C., Maumus, F., Toghe, T. *et al.* (2014) The genome of the stress-tolerant wild tomato species *Solanum pennellii*. *Nature Genetics*, **46**, 1034–1038.
- Cabanettes, F. & Klopp, C. (2018) D-GENIES: dot plot large genomes in an interactive, efficient and simple way. *PeerJ*, **6**, e4958. Available at: <https://peerj.com/articles/4958>
- Chakraborty, M., Baldwin-Brown, J.G., Long, A.D. & Emerson, J.J. (2016) Contiguous and accurate de novo assembly of metazoan genomes with modest long read coverage. *Nucleic Acids Research*, **44**, e147.
- Chang, S.B., Yang, T.J., Datema, E., van Vugt, J., Vosman, B., Kuipers, A. *et al.* (2008) FISH mapping and molecular organization of the major repetitive sequences of tomato. *Chromosome Research*, **16**, 919–933.
- Chen, Y., Nie, F., Xie, S.-Q., Zheng, Y.-F., Dai, Q., Bray, T. *et al.* (2021) Efficient assembly of nanopore reads via highly accurate and intact error correction. *Nature Communications*, **12**, 60.
- Cheng, H., Concepcion, G.T., Feng, X., Zhang, H. & Li, H. (2021) Haplotype-resolved de novo assembly using phased assembly graphs with hifiasm. *Nature Methods*, **18**, 170–175.

- Chitwood-Brown, J., Vallad, G.E., Lee, T.G. & Hutton, S.F. (2021) Characterization and elimination of linkage-drag associated with Fusarium wilt race 3 resistance genes. *Theoretical and Applied Genetics*, **1**, 3.
- Choi, K., Zhao, X., Tock, A.J., Lambing, C., Underwood, C.J., Hardcastle, T.J. et al. (2018) Nucleosomes and DNA methylation shape meiotic DSB frequency in Arabidopsis thaliana transposons and gene regulatory regions. *Genome Research*, **28**, 532–546.
- Costa, J.M. & Heuvelink, E. (2018) The global tomato industry. In: *Tomatoes*. CABI, pp. 1–26.
- Cui, Y., Cui, Z., Xu, J., Hao, D., Shi, J., Wang, D. et al. (2020) NG-Circos: next-generation Circos for data visualization and interpretation. *NAR Genomics and Bioinformatics*, **2**, lqaa069.
- Danecek, P., Auton, A., Abecasis, G., Albers, C.A., Banks, E., DePristo, M.A. et al. (2011) The variant call format and VCFtools. *Bioinformatics*, **27**, 2156–2158.
- Danecek, P., Bonfield, J.K., Liddle, J., Marshall, J., Ohan, V., Pollard, M.O. et al. (2021) Twelve years of SAMtools and BCFtools. *Gigascience*, **10**, giab008.
- De Haas, L.S., Koopmans, R., Lelivelt, C.L.C., Ursem, R., Dirks, R. & James, G.V. (2017) Low-coverage resequencing detects meiotic recombination pattern and features in tomato RILs. *DNA Research*, **24**, 549–558.
- Demirci, S., van Dijk, A.D.J., Sanchez Perez, G., Aflitos, S.A., de Ridder, D. & Peters, S.A. (2017) Distribution, position and genomic characteristics of crossovers in tomato recombinant inbred lines derived from an interspecific cross between *Solanum lycopersicum* and *Solanum pimpinellifolium*. *The Plant Journal*, **89**, 554–564.
- Dumschott, K., Schmidt, M.H.W., Chawla, H.S., Snowdon, R. & Usadel, B. (2020) Oxford Nanopore sequencing: new opportunities for plant genomics? *Journal of Experimental Botany*, **71**, 5313–5322.
- Foolad, M.R., Stoltz, T., Dervinis, C., Rodriguez, R.L. & Jones, R.A. (1997) Mapping QTLs conferring salt tolerance during germination in tomato by selective genotyping. *Molecular Breeding*, **3**, 269–277.
- Ganal, M.W., Lapitan, N.L. & Tanksley, S.D. (1991) Macrostructure of the tomato telomeres. *Plant Cell*, **3**, 87–94.
- Gao, L., Gonda, I., Sun, H., Ma, Q., Bao, K., Tieman, D.M. et al. (2019) The tomato pan-genome uncovers new genes and a rare allele regulating fruit flavor. *Nature Genetics*, **51**, 1044–1051.
- Ghurye, J., Rhie, A., Walenz, B.P., Schmitt, A., Selvaraj, S., Pop, M. et al. (2019) Integrating Hi-C links with assembly graphs for chromosome-scale assembly. *PLoS Computational Biology*, **15**, e1007273. <https://journals.plos.org/ploscompbiol/article?id=10.1371/journal.pcbi.1007273>
- Goel, M., Sun, H., Jiao, W.B. & Schneeberger, K. (2019) SyRI: finding genomic rearrangements and local sequence differences from whole-genome assemblies. *Genome Biology*, **20**, 277. <https://doi.org/10.1186/s13059-019-1911-0> [Accessed July 4, 2021].
- Healey, A., Furtado, A., Cooper, T. & Henry, R.J. (2014) Protocol: a simple method for extracting next-generation sequencing quality genomic DNA from recalcitrant plant species. *Plant Methods*, **10**, 21.
- Hon, T., Mars, K., Young, G., Tsai, Y.-C., Karalius, J.W., Landolin, J.M. et al. (2020) Highly accurate long-read HiFi sequencing data for five complex genomes. *Scientific Data*, **7**, 399.
- Hosmani, P.S., Flores-Gonzalez, M., van de Geest, H., Maumus, F., van Bakker, L., Schijlen, E. et al. (2019) An improved de novo assembly and annotation of the tomato reference genome using single-molecule sequencing, Hi-C proximity ligation and optical maps. *bioRxiv*, 767764. <https://doi.org/10.1101/767764>.
- Jo, S.-H., Koo, D.-H., Kim, J.F., Hur, C.-G., Lee, S., Yang, T. et al. (2009) Evolution of ribosomal DNA-derived satellite repeat in tomato genome. *BMC Plant Biology*, **9**, 42. <https://pmc/articles/PMC2679016/>
- Kim, H.T. & Lee, J.M. (2018) Organellar genome analysis reveals endosymbiotic gene transfers in tomato. *PLoS One*, **13**, e0202279.
- Kolmogorov, M., Yuan, J., Lin, Y. & Pevzner, P.A. (2019) Assembly of long, error-prone reads using repeat graphs. *Nature Biotechnology*, **37**, 540–546. <https://www.nature.com/articles/s41587-019-0072-8>
- Koren, S., Schatz, M.C., Walenz, B.P., Martin, J., Howard, J.T., Ganapathy, G. et al. (2012) Hybrid error correction and de novo assembly of single-molecule sequencing reads. *Nature Biotechnology*, **30**, 693–700.
- Lanfermeijer, F.C., Dijkhuis, J., Sturre, M.J.G., De Haan, P. & Hille, J. (2003) Cloning and characterization of the durable tomato mosaic virus resistance gene Tm-2 from *Lycopersicon esculentum*. *Plant Molecular Biology*, **52**, 1037–1049.
- Lanfermeijer, F.C., Warmink, J. & Hille, J. (2005) The products of the broken Tm-2 and the durable Tm-22 resistance genes from tomato differ in four amino acids. *Journal of Experimental Botany*, **56**, 2925–2933.
- Lhuissier, F.G.P., Offenber, H.H., Wittich, P.E., Vischer, N.O.E. & Heyting, C. (2007) The mismatch repair protein MLH1 marks a subset of strongly interfering crossovers in tomato. *Plant Cell*, **19**, 862–876.
- Li, H. (2011) A statistical framework for SNP calling, mutation discovery, association mapping and population genetical parameter estimation from sequencing data. *Bioinformatics*, **27**, 2987–2993. <https://pmc/articles/PMC3198575/>
- Li, H. (2018) Minimap2: pairwise alignment for nucleotide sequences. *Bioinformatics*, **34**, 3094–3100.
- Li, H. & Durbin, R. (2009) Fast and accurate short read alignment with Burrows-Wheeler transform. *Bioinformatics*, **25**, 1754–1760. <https://pubmed.ncbi.nlm.nih.gov/19451168/>
- Li, J., Liu, L., Bai, Y., Zhang, P., Finkers, R., Du, Y. et al. (2010) Seedling salt tolerance in tomato. *Euphytica*, **178**, 403–414.
- Lin, T., Zhu, G., Zhang, J., Xu, X., Yu, Q., Zheng, Z. et al. (2014) Genomic analyses provide insights into the history of tomato breeding. *Nature Genetics*, **46**, 1220–1226.
- Liu, Y., Du, H., Li, P., Shen, Y., Peng, H., Liu, S. et al. (2020) Pan-genome of wild and cultivated soybeans. *Cell*, **182**, 162–176.e13.
- Marçais, G. & Kingsford, C. (2011) A fast, lock-free approach for efficient parallel counting of occurrences of k-mers. *Bioinformatics*, **27**, 764–770.
- Mascher, M., Wicker, T., Jenkins, J., Plott, C., Lux, T., Shin Koh, C. et al. (2021) Long-read sequence assembly: a technical evaluation in barley. *Plant Cell*, **33**, 1888–1906.
- Michael, T.P., Jupe, F., Bemm, F., Motley, S.T., Sandoval, J.P., Lanz, C. et al. (2018) High contiguity Arabidopsis thaliana genome assembly with a single nanopore flow cell. *Nature Communications*, **9**, 541
- Mikheenko, A., Pribelski, A., Saveliev, V., Antipov, D. & Gurevich, A. (2018) Versatile genome assembly evaluation with QUAST-LG. *Bioinformatics*, **34**, i142–i150. <https://academic.oup.com/bioinformatics/article/34/13/i142/5045727>
- Naish, M., Alonge, M., Wlodzimierz, P., Tock, A.J., Abramson, B.W., Schmucker, A. et al. (2021) The genetic and epigenetic landscape of the Arabidopsis centromeres. *Science*, **374**, abi7489.
- Nurk, S., Koren, S., Rhie, A., Rautiainen, M., Bzikadze, A.V., Mikheenko, A. et al. (2021) The complete sequence of a human genome. *bioRxiv*, 2021.05.26.445798. <https://doi.org/10.1101/2021.05.26.445798>.
- Nurk, S., Walenz, B.P., Rhie, A., Vollger, M.R., Logsdon, G.A., Grothe, R. et al. (2020) HiCanu: accurate assembly of segmental duplications, satellites, and allelic variants from high-fidelity long reads. *Genome Research*, **30**, 1291–1305.
- Ou, S., Chen, J. & Jiang, N. (2018) Assessing genome assembly quality using the LTR Assembly Index (LAI). *Nucleic Acids Research*, **46**, e126. <https://github.com/oushujun/>
- Payne, A., Holmes, N., Rakyen, V. & Loose, M. (2019) Bulkvis: a graphical viewer for Oxford nanopore bulk FAST5 files. *Bioinformatics*, **35**, 2193–2198.
- Pedersen, B.S., Collins, R.L., Talkowski, M.E. & Quinlan, A.R. (2017) Indexcov: fast coverage quality control for whole-genome sequencing. *Gigascience*, **6**, gix090.
- Pedersen, B.S. & Quinlan, A.R. (2018) Mosdepth: quick coverage calculation for genomes and exomes. *Bioinformatics*, **34**, 867–868.
- Pelham, J. (1966) Resistance in tomato to tobacco mosaic virus. *Euphytica*, **15**, 258–267.
- Peralta, I.E., Spooner, D.M. & Knapp, S. (2008) *Taxonomy of wild tomatoes and their relatives (Solanum sect. Lycopersicoides, sect. Juglandifolia, sect. Lycopersicon ; Solanaceae)*, American Society of Plant Taxonomists.
- Perry, K.L. & Palukaitis, P. (1990) Transcription of tomato ribosomal DNA and the organization of the intergenic spacer. *Molecular Genetics and Genomics*, **221**, 102–112.
- Powell, A.F., Courtney, L.E., Schmidt, M.H.-W., Feder, A., Vogel, A., Xu, Y. et al. (2020) A *Solanum lycopersicoides* reference genome facilitates biological discovery in tomato. *bioRxiv*, 2020.04.16.039636. <https://doi.org/10.1101/2020.04.16.039636>.
- Qin, P., Lu, H., Du, H., Wang, H., Chen, W., Chen, Z. et al. (2021) Pan-genome analysis of 33 genetically diverse rice accessions reveals hidden genomic variations. *Cell*, **184**, 3542–3558.e16.

- Quinlan, A. & Hall, I. (2010) BEDTools: a flexible suite of utilities for comparing genomic features. *Bioinformatics*, **26**, 841–842.
- Robinson, J.T., Thorvaldsdóttir, H., Winckler, W., Guttman, M., Lander, E.S., Getz, G. *et al.* (2011) Integrative genomics viewer. *Nature Biotechnology*, **29**, 24–26.
- Ross, K.J., Franz, P. & Jones, G.H. (1996) A light microscopic atlas of meiosis in *Arabidopsis thaliana*. *Chromosome Research*, **4**, 507–516.
- Rubio, F., Alonso, A., Garcia-Martinez, S. & Ruiz, J.J. (2016) Introgression of virus-resistance genes into traditional Spanish tomato cultivars (*Solanum lycopersicum* L.): Effects on yield and quality. *Scientia Horticulturae*, **198**, 183–190.
- Sato, S., Tabata, S., Hirakawa, H., Asamizu, E., Shirasawa, K., Isobe, S. *et al.* (2012) The tomato genome sequence provides insights into fleshy fruit evolution. *Nature*, **485**, 635–641.
- Schmidt, M.H.-W., Vogel, A., Denton, A.K., Istace, B., Wormit, A., van de Geest, H. *et al.* (2017) De Novo Assembly of a New *Solanum pennellii* accession Using Nanopore Sequencing. *Plant Cell*, **29**, 2336–2348.
- Schmidt-Puchta, W., Günther, I. & Sânger, H.L. (1989) Nucleotide sequence of the intergenic spacer (IGS) of the tomato ribosomal DNA. *Plant Molecular Biology*, **13**, 251–253. <https://link.springer.com/article/10.1007/BF00016143>
- Schouten, H.J., Tikunov, Y., Verkerke, W., Finkers, R., Bovy, A., Bai, Y. *et al.* (2019) breeding has increased the diversity of cultivated tomato in the Netherlands. *Frontiers in Plant Science*, **10**, 1606.
- Seppy, M., Manni, M. & Zdobnov, E.M. (2019) BUSCO: Assessing Genome Assembly and Annotation Completeness. *Methods in Molecular Biology*, **1962**, 227–245.
- Simão, F.A., Waterhouse, R.M., Ioannidis, P., Kriventseva, E.V. & Zdobnov, E.M. (2015) BUSCO: assessing genome assembly and annotation completeness with single-copy orthologs. *Bioinformatics*, **31**, 3210–3212.
- Tanksley, S.D., Bernachi, D., Beck-Bunn, T., Emmatty, D., Eshed, Y., Inai, S. *et al.* (1998) Yield and quality evaluations on a pair of processing tomato lines nearly isogenic for the Tm2a gene for resistance to the tobacco mosaic virus. *Euphytica*, **99**, 77–83.
- Underwood, C.J., Choi, K., Lambing, C., Zhao, X., Serra, H., Borges, F. *et al.* (2018) Epigenetic activation of meiotic recombination near *Arabidopsis thaliana* centromeres via loss of H3K9me2 and non-CG DNA methylation. *Genome Research*, **28**, 519–531.
- Vaillancourt, B. & Buell, C.R. (2019) High molecular weight DNA isolation method from diverse plant species for use with Oxford Nanopore sequencing. *bioRxiv*, 783159. Available at: <https://doi.org/10.1101/783159>
- VanBuren, R., Bryant, D., Edger, P.P., Tang, H., Burgess, D., Challabathala, D. *et al.* (2015) Single-molecule sequencing of the desiccation-tolerant grass *Oropetium thomaeum*. *Nature*, **527**, 508–511.
- Vaser, R., Sović, I., Nagarajan, N. & Sikić, M. (2017) Fast and accurate de novo genome assembly from long uncorrected reads. *Genome Research*, **27**, 737–746.
- Vilanova, S., Alonso, D., Gramazio, P., Plazas, M., Garcia-Fortea, E., Ferrante, P. *et al.* (2020) SILEX: a fast and inexpensive high-quality DNA extraction method suitable for multiple sequencing platforms and recalcitrant plant species. *Plant Methods*, **16**, 110.
- Vollger, M.R., Logsdon, G.A., Audano, P.A., Sulovari, A., Porubsky, D., Peluso, P. *et al.* (2020) Improved assembly and variant detection of a haploid human genome using single-molecule, high-fidelity long reads. *Annals of Human Genetics*, **84**, 125–140.
- Wang, J., Chen, T., Han, M., Qian, L., Li, J., Wu, M. *et al.* (2020) Plant NLR immune receptor Tm-22 activation requires NB-ARC domain-mediated self-association of CC domain. *PLoS Pathogens*, **16**, e1008475.
- Zapata, L., Ding, J., Willing, E.M., Hartwig, B., Bezdán, D., Jiao, W.-B. *et al.* (2016) Chromosome-level assembly of *Arabidopsis thaliana* Ler reveals the extent of translocation and inversion polymorphisms. *Proceedings of the National Academy of Sciences of the United States of America*, **113**, E4052–E4060.
- Wang, Y., Van Rens, W.M.J., Zaidan, M.W.A.M. & Underwood, C.J. (2021) Meiosis in crops: from genes to genomes. *Journal of Experimental Botany*, **72**, 6091–6109.
- Zapata, L., Ding, J., Willing, E.M. *et al.* (2016) Chromosome-level assembly of *Arabidopsis thaliana* Ler reveals the extent of translocation and inversion polymorphisms. *Proceedings of the National Academy of Sciences of the United States of America*, **113**, E4052–E4060. Available at: <http://www.ncbi.nlm.nih.gov/pubmed/27354520> [Accessed November 26, 2017].
- Zhao, M., Ku, J.-C., Liu, B., Yang, D., Yin, L., Ferrell, T.J. *et al.* (2021) The mop1 mutation affects the recombination landscape in maize. *Proceedings of the National Academy of Sciences of the United States of America*, **118**, e2009475118.
- Zhong, X.B., Franz, P.F., Van Eden, J.W., Ramanna, M.S., Van Kammen, A., Zabel, P. *et al.* (1998) FISH studies reveal the molecular and chromosomal organization of individual telomere domains in tomato. *The Plant Journal*, **13**, 507–517.
- Zhu, G., Wang, S., Huang, Z., Zhang, S., Liao, Q., Zhang, C. *et al.* (2018) Rewiring of the fruit metabolome in tomato breeding. *Cell*, **172**, 249–261.e12.